

# Conserved number fluctuations under global rotation in a hadron resonance gas model

Gaurav Mukherjee<sup>1,2a</sup>, Dipanwita Dutta<sup>1,2b</sup>, and Dipak Kumar Mishra<sup>1c</sup>

<sup>1</sup> Nuclear Physics Division, Bhabha Atomic Research Centre, Mumbai - 400085, INDIA

<sup>2</sup> Homi Bhabha National Institute, Anushaktinagar, Mumbai - 400094, INDIA

the date of receipt and acceptance should be inserted later

**Abstract.** Net-baryon number, net-charge and net-strangeness fluctuations measured in ultra-relativistic heavy-ion collisions may reveal details and insights into the quark-hadron transition, hadrochemical freeze-out and possibly aid in the search of the QCD critical point. By scanning in collision energy, current and upcoming heavy-ion facilities aim to explore the finite density regime where the critical point may lie. Effects due to rotation are also expected in case of peripheral collisions and we report on conserved number susceptibilities as calculated in the hadron resonance gas model augmented by a global angular velocity. Since these quantities are directly related to the experimentally measurable moments of the corresponding distributions our results show the possible impact of vorticity on the theoretical baseline and should be useful for referencing with experimental data and QCD-based calculations.

**PACS.** 12.38.Mh Quark-gluon plasma – 12.38.Gc HRG Model

## 1 Introduction

Properties of QCD matter under extreme conditions are being probed at Relativistic Heavy Ion Collider (RHIC) and Large Hadron Collider (LHC), and will be further studied in upcoming facilities like Nuclotron-based Ion Collider fAcility (NICA), JINR, Dubna and the Facility for Antiproton, Ion Research (FAIR), GSI, Darmstadt and Heavy-Ion program at Japan Proton Accelerator Research Complex (J-PARC-HI), Japan. In the peripheral nucleus-nucleus collisions, the created fireball may sustain rapid rotation for which the angular momentum is generated as a result of the initial non-zero impact parameter,  $b$ . In such heavy-ion collisions (HIC), the two colliding nuclei carry a total angular momentum  $J \propto b\sqrt{s_{NN}}$ , where  $\sqrt{s_{NN}}$  is the nucleon-nucleon center-of-mass energy. Though most of the total angular momentum is carried away by the spectators, a finite amount of the order of  $10^4$ -  $10^5\hbar$  remains in the fireball with local angular velocity in the range 0.01-0.1 GeV [1–5]. This scenario is experimentally supported by the STAR experiment at RHIC with the measurement of a non-zero value of  $\Lambda$  and  $\bar{\Lambda}$  polarization which can be translated to large values of the vorticity or angular velocity,  $\omega \sim (9 \pm 1) \times 10^{21} s^{-1} \sim 0.05m_\pi$  [6]. In addition to temperature  $T$  and baryon chemical potential  $\mu_B$ , vorticity or angular velocity ( $\omega$ ) acts as an additional control

parameter and should influence the thermodynamics and phase diagram in non-trivial ways [7–10].

Many interesting phenomena can occur in rotating QCD matter. As examples, chiral vortical effect [11–13] and chiral vortical wave [14] can be induced due to fluid rotation. On the other hand, the rotational counterpart of magnetic catalysis, i.e., the formation of the scalar condensate which leads to spontaneous breaking of chiral symmetry, is also being investigated [15]. Thus, it is important to consider the effect of rotation while studying the properties of the medium formed in HICs. The first-principles study of QCD in rotating frames by using lattice simulations has seen recent interest [16, 17]. However the notorious sign problem that plagues the finite density calculations returns in the case of rotating matter due to the effective chemical potential induced by the latter. This motivates the application of QCD-based models to probe dense rotating QCD matter.

The QCD phase transitions are of a crossover type at small values of  $\mu_B$  which is established by lattice QCD [18–22] but is expected to become first order at higher values of  $\mu_B$  as corroborated by various effective model calculations [23–25]. The existence of a critical end point (CEP) is thus expected at the termination of the first-order phase transition line [26, 27]. Locating this CEP is an exciting frontier in experimental as well as theoretical high energy nuclear physics (see Ref. [28] for a recent review).

The presence of CEP would lead to large correlation lengths and result in divergent fluctuations in various thermodynamic quantities. These may be accessed from the

<sup>a</sup> phy.res.gaurav.m@gmail.com

<sup>b</sup> ddutta08@hbni.ac.in

<sup>c</sup> dkmishra@barc.gov.in

event-by-event fluctuations analyses of the quantum numbers or conserved charges, *viz.* net-baryon number, net-charge and net-strangeness, obtained from heavy-ion collision data. This will be possible if the CEP lies close to the freeze-out curve and the large fluctuations survive in remnant form until freeze-out to a sufficient level. The moments (more accurately, cumulants) of such distributions have been proposed as sensitive indicators of a transition between hadronic and quark-gluon matter and may direct to the location of the CEP [29–34].

The thermal properties of hot and dense QCD matter are described well by the hadron resonance gas (HRG) model. The experimental fits yield the freeze-out parameters and these show a consistent behavior for different collision energies [35]. The HRG model also provides the theoretical baseline against which the large fluctuations and correlations in the vicinity of the critical point may be starkly contrasted with experimental data and independent QCD-based calculations [34–39]. Recently, the deconfinement transition of rotating hot and dense matter has been studied within the HRG model [7]. Here we shall explore the higher moments of fluctuations of net-baryon number, net-charge and net-strangeness for a rotating QCD medium and their dependence on the collision energy. We perform our analysis in the framework of a rotating HRG model to estimate the different thermodynamic quantities such as pressure, entropy density as well as susceptibilities and their ratios [7, 15]. Calculations including the effects of rotation are shown for the ratios of quartic and quadratic (kurtosis), cubic and quadratic (skewness) as well as quadratic charge fluctuations normalized to their mean value along a phenomenologically determined freeze-out curve in HICs [32, 35].

In Sec. 2 we describe a reformulation of the standard HRG model, as modified due to the inclusion of rotation. This is then used to compute the equation of state via thermodynamic variables like pressure, entropy density and energy density. We report the main results with regard to the susceptibilities and their ratios in Sec. 3. Their phenomenological utility via connection to the observable moments of the conserved charge distributions is discussed as well. Finally in Sec. 4, we summarize our findings.

## 2 Rotating HRG model: Bulk properties

In the HRG model [36], the confined phase of QCD matter is modeled by an ideal relativistic gas of all known hadrons and resonances. It has been used alongside ab initio lattice QCD treatments and both are found to be mutually consistent in their overlap region of validity.

Under the coordinate transformation suitable for a rigid global rotation, all local quantities can be expressed as functions of the co-rotating coordinates,  $x^\mu$ , in the non-inertial rotating frame of reference instead of  $\tilde{x}^\mu$  in the

rest (lab) frame. The corresponding metric can be read as

$$g_{\mu\nu} = \eta_{ab} \frac{\partial \tilde{x}^a}{\partial x^\mu} \frac{\partial \tilde{x}^b}{\partial x^\nu} = \begin{pmatrix} 1 - (x^2 + y^2)\omega^2 & y\omega & -x\omega & 0 \\ y\omega & -1 & 0 & 0 \\ -x\omega & 0 & -1 & 0 \\ 0 & 0 & 0 & -1 \end{pmatrix}, \tag{1}$$

with the Minkowskian metric taken as  $\eta = \text{diag}(1, -1, -1, -1)$ . To deal with the fermions we introduce the vierbein,  $\eta_{ab} = e_a^\mu e_b^\nu g^{\mu\nu}$ , and adopt

$$e_0^t = e_1^x = e_2^y = e_3^z = 1, \quad e_0^x = y\omega, \quad e_0^y = -x\omega, \tag{2}$$

taking all other components zero.

The explicit calculations [7] yield the pressure  $p_i^{B/M}$  for  $i^{\text{th}}$  baryon (superscript  $B$ , upper signs) or meson (superscript  $M$ , lower signs), and is given by

$$p_i^{B/M} = \pm \frac{T}{8\pi^2} \sum_{l=-\infty}^{\infty} \int dk_r^2 \int dk_z \sum_{\nu=l}^{l+2s_i} J_\nu^2(k_r r) \ln(1 \pm e^{-(E_i - \mu_i)/T}). \tag{3}$$

Here  $J_\nu^2(k_r r)$  is the (squared) Bessel function and  $\mu_i = B_i \mu_B + S_i \mu_S + Q_i \mu_Q$  is the total chemical potential with  $B_i$ ,  $S_i$  and  $Q_i$  the respective baryon number, strangeness and electric-charge of the  $i^{\text{th}}$  particle and the  $\mu_B$ ,  $\mu_S$  and  $\mu_Q$  are the corresponding chemical potentials. In order to implement the conservation laws for strangeness and electric charge, we have introduced the strangeness and the electric charge chemical potentials for the complete system.  $\mu_S$  and  $\mu_Q$  have non-zero (finite) values to obtain net strangeness equal to zero and baryon number to charge ratio  $N_B/N_Q \simeq 2.52$ , which comes from beta-equilibrium with the Coulomb interaction in the heavy-ion collisions. The single-particle energy levels are given as

$$E_i = \sqrt{k_r^2 + k_z^2 + m_i^2} - (l + s_i)\omega, \tag{4}$$

where  $s_i$  and  $m_i$  are the spin and mass of the  $i^{\text{th}}$  particle respectively. The final term behaves as an effective chemical potential due to rotation. We have incorporated all hadrons listed in particle data book [40] up to an ultraviolet mass cut of  $\Lambda = 1.5$  GeV to save numerical cost [35].

The causality condition prohibits the formation of unphysical condensates by forbidding the  $(l + s)\omega$  term to become greater than the ‘free-particle’ part of the energy dispersion  $\sqrt{k_r^2 + k_z^2 + m_i^2}$ . Imposing a boundary condition on the wave-function to be normalized within  $r \leq R$ , the causality requires  $R\omega \leq 1$ . The leading discretization effect of momenta from causality bound is in the low momentum region and thus an infrared cut-off for the  $k_r$  integration is introduced [7], which is defined as,  $\Lambda_l^{IR} = \zeta_{l,1}\omega$ . Here  $\zeta_{l,1}$  is the first zero of the Bessel function:  $J_l(\zeta_{l,1}) = 0$ . The  $k_r$  integration in Eq. 3 is then redefined as,

$$\int dk_r^2 \rightarrow \int_{(\Lambda_l^{IR})^2} dk_r^2. \tag{5}$$

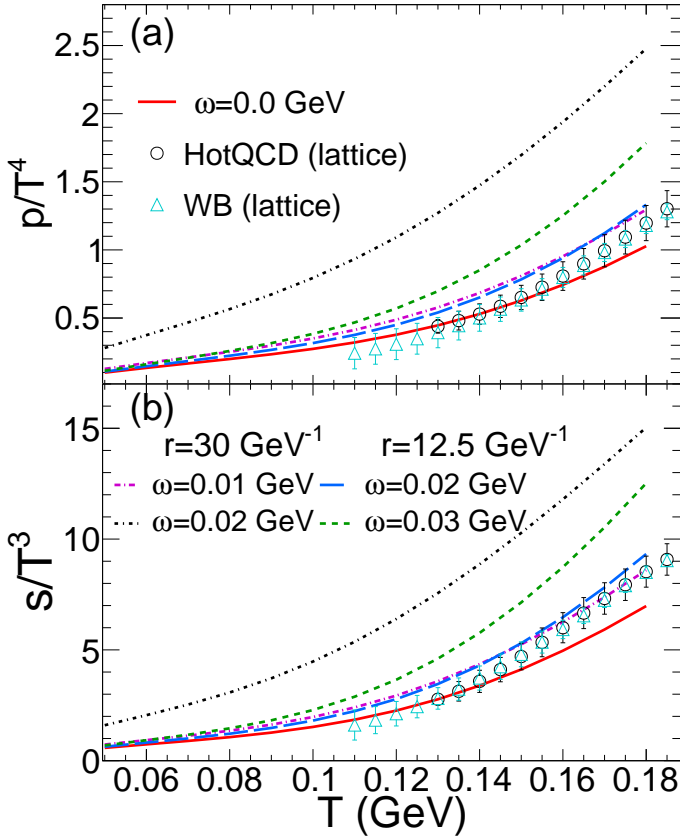


**Fig. 1.** (Top) Scaled pressure  $p/T^4$  and (bottom) entropy density  $s/T^3$  as a function of the temperature  $T$  for different angular velocity  $\omega$  at  $\mu = 0$ . The open circle and cyan triangle symbols are for HotQCD [41] and WB [42] lattice data respectively calculated at  $\mu = 0$ .

Figure 1 shows the effect of rotation ( $\omega$ ) on thermodynamic variables like pressure  $p/T^4$  (top panel) and entropy density  $s/T^3$  (bottom panel) as a function of temperature  $T$ . The HRG results with and without rotation are compared with the lattice QCD results of the Hot-QCD Collaboration [41] and the Wuppertal-Budapest (WB) Collaboration [42] shown in the same figure. Here we have considered two different centrality classes in HICs: (i) central collisions where the fireball radius  $R = 30$  GeV $^{-1}$  (corresponds to  $R = 6$  fm) and (ii) peripheral collisions where  $R = 12.5$  GeV $^{-1}$  (corresponds to  $R = 2.5$  fm) [43]. In Fig. 1, we have used  $r = 30$  GeV $^{-1}$  ( $r = 12.5$  GeV $^{-1}$ ) for central (peripheral) collisions respectively. It is observed that in both cases, the pressure and entropy density increases with rotation  $\omega$ . The value of the angular velocity  $\omega = 0.01 - 0.04$  GeV, considered in this study, lies in the range that is expected at freeze-out in heavy-ion collisions [2]. The causality condition  $R\omega \leq 1$  is respected too, for this range. It is observed that  $p/T^4$  and  $s/T^3$  increase with  $T$  and there is a rising trend for both with increasing radius  $r$ . Similar behavior was also noted in Ref. [7]. The lattice results at lower  $T < 150$  MeV are well described by ideal HRG without taking rotation into account. The two graphs which correspond to  $r = 12.5$

GeV $^{-1}$  (blue dash) and  $r = 30$  GeV $^{-1}$  (black dotted) for  $\omega = 0.02$  GeV are shown in Fig 1. In this study, we consider the highest possible  $r$  ( $r \leq R$ ) for both peripheral ( $r = 12.5$  GeV $^{-1}$ ) and central ( $r = 30$  GeV $^{-1}$ ) collisions to investigate the maximum effect of rotation  $\omega$  on the fluctuations (susceptibilities).

### 3 Observables: Moments and Susceptibilities

In HRG model calculations, susceptibilities are defined as derivatives of the (scaled) pressure  $p = -f$  with respect to the (scaled) chemical potential in the following way [44]

$$\chi_x^k = \frac{\partial^k (\Sigma_i p_i / T^4)}{\partial (\mu_x / T)^k}, \quad (6)$$

where  $k$  is the order of derivatives and the conserved quantum numbers such as baryon number, strangeness, and electric-charge are represented by  $x$ . From the definition of the grand canonical partition function, one can show that susceptibilities are related to the cumulants of the event-by-event multiplicity distributions which are measurable in the heavy-ion experiments via the relations,

$$\chi^1 = \frac{1}{VT^3} \langle N \rangle, \quad \chi^2 = \frac{1}{VT^3} \langle (\Delta N)^2 \rangle, \quad \chi^3 = \frac{1}{VT^3} \langle (\Delta N)^3 \rangle,$$

$$\chi^4 = \frac{1}{VT^3} \langle (\Delta N)_c^4 \rangle \equiv \langle (\Delta N)^4 \rangle - 3 \langle (\Delta N)^2 \rangle^2,$$

$$\chi^5 = \frac{1}{VT^3} \langle (\Delta N)_c^5 \rangle$$

$$\equiv \langle (\Delta N)^5 \rangle - 10 \langle (\Delta N)^3 \rangle \langle (\Delta N)^2 \rangle,$$

$$\chi^6 = \frac{1}{VT^3} \langle (\Delta N)_c^6 \rangle$$

$$\equiv \langle (\Delta N)^6 \rangle - 15 \langle (\Delta N)^4 \rangle \langle (\Delta N)^2 \rangle - 10 \langle (\Delta N)^3 \rangle^2$$

$$+ 30 \langle (\Delta N)^2 \rangle^3. \quad (7)$$

Here,  $N$  is the number of the measured particles or conserved charges.  $\Delta N = N - \langle N \rangle$  is the fluctuation around the event-averaged mean  $\langle N \rangle$ . The ratios of the susceptibilities yield the products of moments as,

$$\frac{\chi^2}{\chi^1} = \frac{\sigma^2}{M}, \quad \frac{\chi^3}{\chi^2} = S\sigma, \quad \frac{\chi^4}{\chi^2} = \kappa\sigma^2, \quad \frac{\chi^6}{\chi^2} = \kappa^H\sigma^4. \quad (8)$$

The mean  $M$ , the variance  $\sigma^2$ , the skewness  $S$ , the kurtosis  $\kappa$  and the hyper-kurtosis  $\kappa^H$  are obtained experimentally from the measured event-by-event multiplicity distributions [45, 46]. These moments characterize the shape of the multiplicity distributions. Equation 8 establishes the relation between the experimentally measurable moments and the theoretically calculable susceptibilities from thermodynamics and this relation is to be utilized to provide the predictions from our modified HRG model. One advantage of measuring the  $\sigma^2/M$ ,  $S\sigma$ , and  $\kappa\sigma^2$  is that the volume dependence of  $M$ ,  $\sigma$ ,  $S$ , and  $\kappa$  cancel out in the ratios; hence theoretical calculations can be directly compared with the experimental measurements.

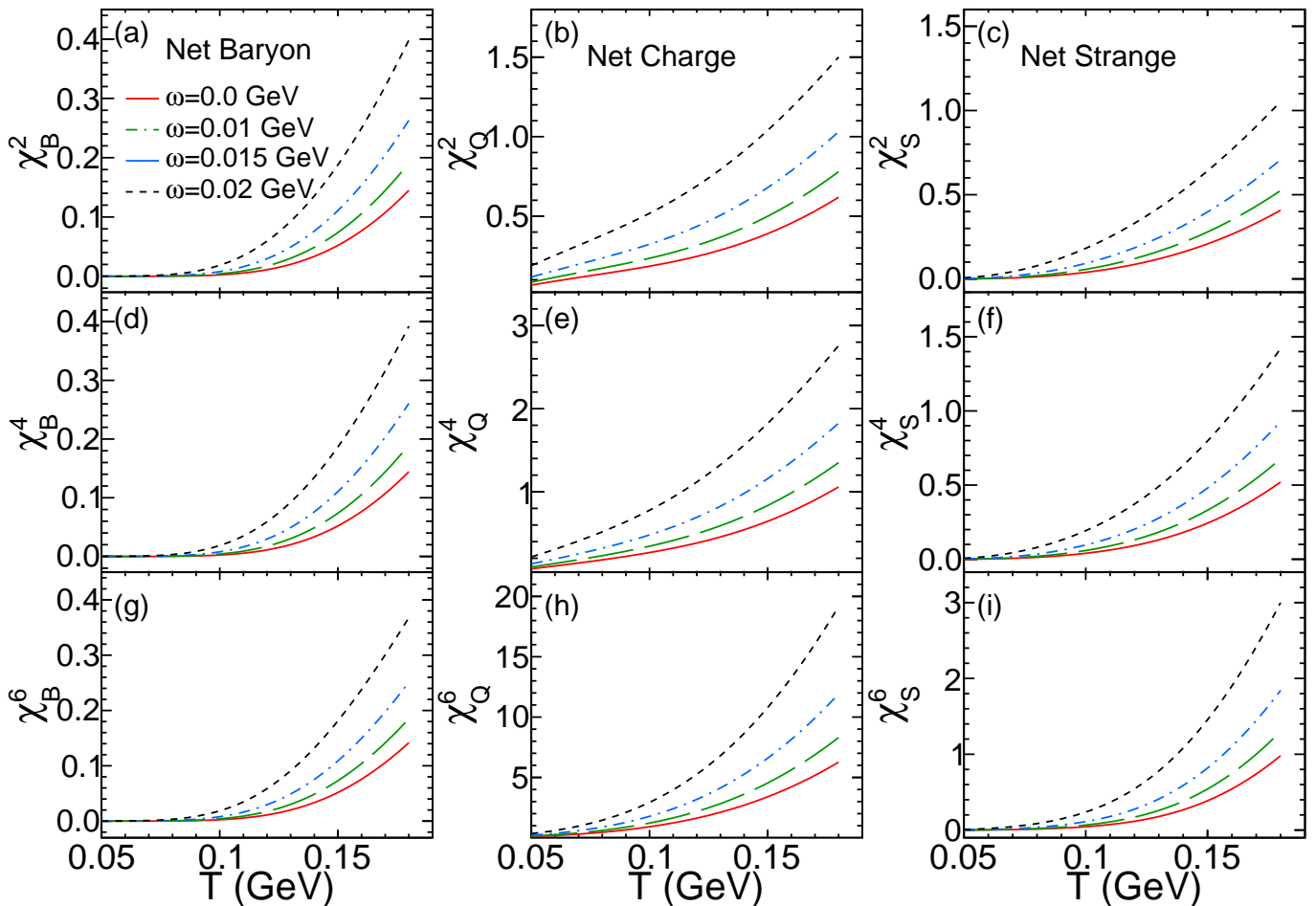


**Fig. 2.**  $\chi^2$  (upper row),  $\chi^4$  (middle row) and  $\chi^6$  (lower row) as a function of the temperature  $T$  for different angular velocity  $\omega$  at  $\mu = 0$  for baryon number (left column), electric charge (middle column) and strangeness (right column).

## 4 Results and Discussions

The susceptibilities are related to ensemble fluctuations of the conserved quantities which can be obtained from event-by-event multiplicity measurements in heavy-ion collision experiments. The study of fluctuations in heavy-ion collisions is an important tool for the experimental determination of the QCD critical point and the first-order phase transition. Figure 2 shows the variation of second-order ( $\chi^2$ ), fourth-order ( $\chi^4$ ) and sixth-order ( $\chi^6$ ) susceptibilities of different conserved charges: baryon number (left column), electric charge (middle column) and strangeness (right column) with temperature  $T$  at chemical potential  $\mu = 0$  for different values of the angular velocity  $\omega$ . The susceptibilities are calculated along the freeze-out curve determined from the universal freeze-out condition on a fixed value of entropy density  $s/T^3 \simeq 7.0$ . The variation of even order susceptibilities corresponding to the conserved charges are similar. However, the absolute values of the higher order susceptibility are generally larger compared to the second order susceptibilities due to the larger weight for higher order. If the chiral crossover is near the freeze-out line on the phase diagram the higher order cumulants for net baryon number and electric charge

fluctuations should show a sharp contrast with the HRG reference values [47].

The equation of state is clearly affected due to rotation (for example, the pressure is shown to behave in accordance with the expected centrifugation as a function of radial distance from the axis of rotation in Ref. [7], also see Fig. 1). By virtue of this influence the susceptibilities also inherit the effects of rotation as observed in our results. The best way to see how rotation impacts these observables is to consider the whole system to be composed of an infinite sequence of coaxial shells or cylindrical surfaces with radii  $r_i \leq R$ ,  $i = 1, 2, 3, \dots$ , and regard one such cylindrical surface at fixed radial distance,  $r$ , as a member of the sub-ensemble (of the ensemble of identical cylindrical systems of radius  $R$ ). Each cylindrical shell is in thermal and chemical (grand canonical) contact and equilibrium with the solid inner core and the remaining outer annular parts of the cylindrical system simultaneously. It is expected that the centrifugation from rotation and boundary effects due to the causality bound will lead to the exchange of conserved charges between the inner core and annular cladding between which the thin shell at  $r_i$  is sandwiched in a biased way or asymmetrically. This

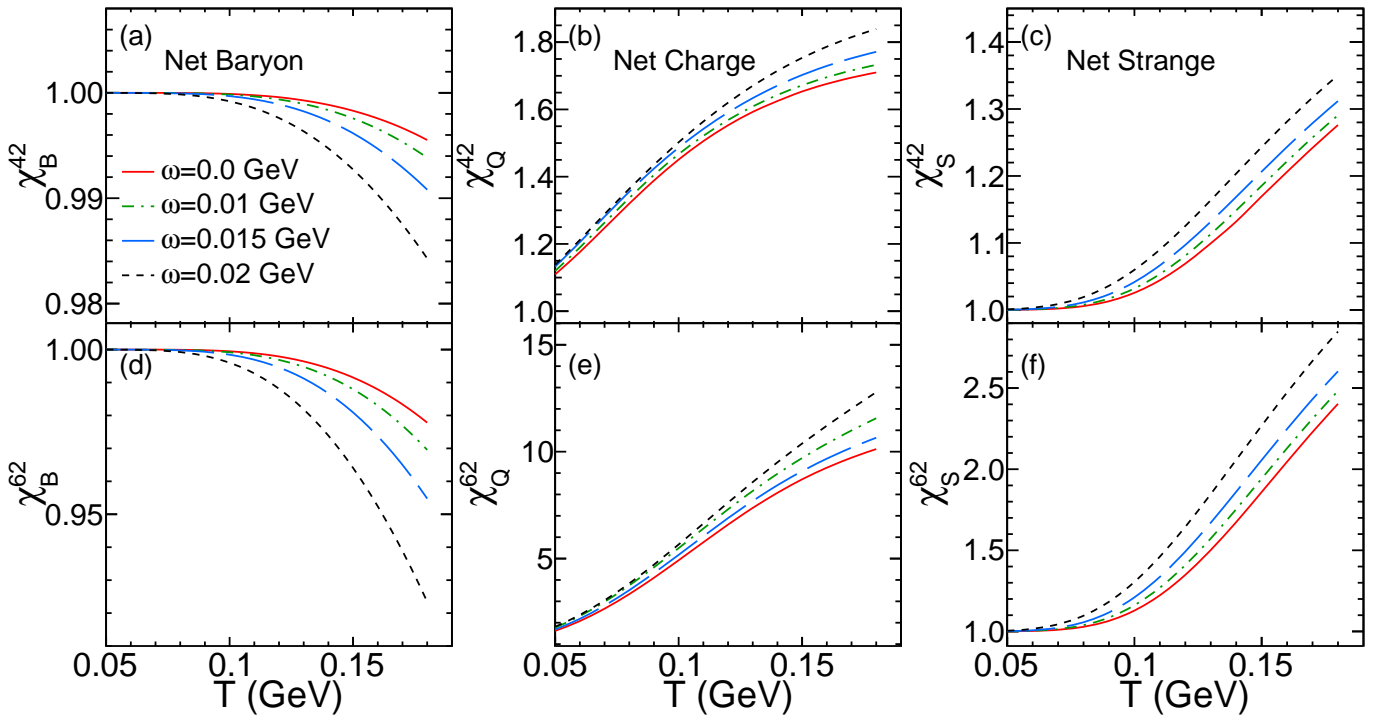


**Fig. 3.**  $\chi^{42} = \chi^4/\chi^2$  (top row) and  $\chi^{62} = \chi^6/\chi^2$  (bottom row) as a function of the temperature  $T$  for different angular velocity  $\omega$  at  $\mu = 0$  for baryon number (left column), electric charge (middle column) and strangeness (right column).

is the likely physical origin of the effects observed here and thus may be attributed to the geometry of the system and the kinematics of its rotation.

In case of HRG model with and without rotation, the susceptibilities increase with temperature  $T$ . At low temperature the contribution to  $\chi_B$  is mainly from proton and neutron. With increase of temperature  $T$  other baryons also start contributing, hence with temperature  $T$  susceptibilities  $\chi_B^2$ ,  $\chi_B^4$ ,  $\chi_B^6$  increase. We also notice that, the susceptibilities increase with rotation  $\omega$  at specific temperature  $T$ . This is because, number density, pressure as well as entropy density increase with  $\omega$  after a specific temperature  $T$ . Similar behavior with temperature  $T$  and rotation  $\omega$  is also observed for  $\chi_Q$  and  $\chi_S$ .

In case of  $\chi_Q$ , the major contributions are from pions and kaons. With increase in temperature more charged particles ( $\rho$ ,  $K^*$ ,  $p$ ,  $\Delta$ , etc.) are produced in the system which contribute to the increase in susceptibilities at higher temperature. Similarly the dominant contribution to the ( $\chi_S$ ) at low temperatures comes from kaons which have strange quantum number  $\pm 1$ . As a result, magnitudes of the susceptibilities ( $\chi_S^2$ ,  $\chi_S^4$ , and  $\chi_S^6$ ) are similar in the low- $T$  region up to 0.1 GeV. At higher temperature, other strange hadrons (e.g.,  $\Sigma$ ,  $\Xi$ ,  $\Omega$ , etc.) having strangeness number  $\pm 2$  and  $\pm 3$  contribute to the higher values of susceptibilities. Hence, at high- $T$ , the higher order susceptibilities ( $\chi_S^6$ ) increase rapidly. So, the rotation effect enhances the fluctuations of the conserved quantities along the freeze-out curve. Figure 3 shows the ratios of susceptibilities ( $\chi^4/\chi^2$ ,  $\chi^6/\chi^2$ ) as a function  $T$  for net-baryon, net-charge and net-strangeness for different values of  $\omega$ .

The net-baryon susceptibilities ratios  $\chi_B^4/\chi_B^2$ ,  $\chi_B^6/\chi_B^2$  decrease as a function of  $T$ . The values are further lowered as we increase  $\omega$ . On the other hand, as in case of net-charge and net-strangeness shows the increasing trend as a function of  $T$ . The ratios are systematically higher with increase in  $\omega$ .

The charge conservation and zero strangeness condition plays an important role in the calculation of the fluctuations in presence of rotation particularly at lower collision energies (higher  $\mu_B$ ) [7]. The strangeness chemical potential  $\mu_S$  grows as  $\mu_B/3$  and compare with the free-out data from the experimental measurements, it is crucial to impose the zero strangeness ( $N_s = 0$ ) and  $N_B/N_Q \simeq 2.52$  condition. Figure 4 shows the susceptibilities ( $\chi^2$ ,  $\chi^4$ , and  $\chi^6$ ) as a function of  $\mu_B$  with and without inclusion of conservation effect along the freeze-out curve which is determined by imposing the fixed value of entropy density  $s/T^3 \simeq 7.0$ . For rotation  $\omega = 0$ ,  $\chi_B^2$ ,  $\chi_B^4$ , and  $\chi_B^6$  are almost same as with and without charge conservation. At  $\omega = 0.02$  GeV, the charge conservation decrease the baryon fluctuations as compared to without conservation. In case of  $\chi_Q$ , conservation has no effect on the charge fluctuations both with and without inclusion of rotation case. In case  $\chi_S$ , the fluctuations are large without charge conservation as compared to the with charge conservation and it is true for both zero and non-zero values for rotation. The charge conservation diminishes the strangeness fluctuations along the freeze-out curve. However, the charge conservation effect is not observed in the ratios of susceptibility ( $\chi^{42}$ ) except strangeness fluctuation case.

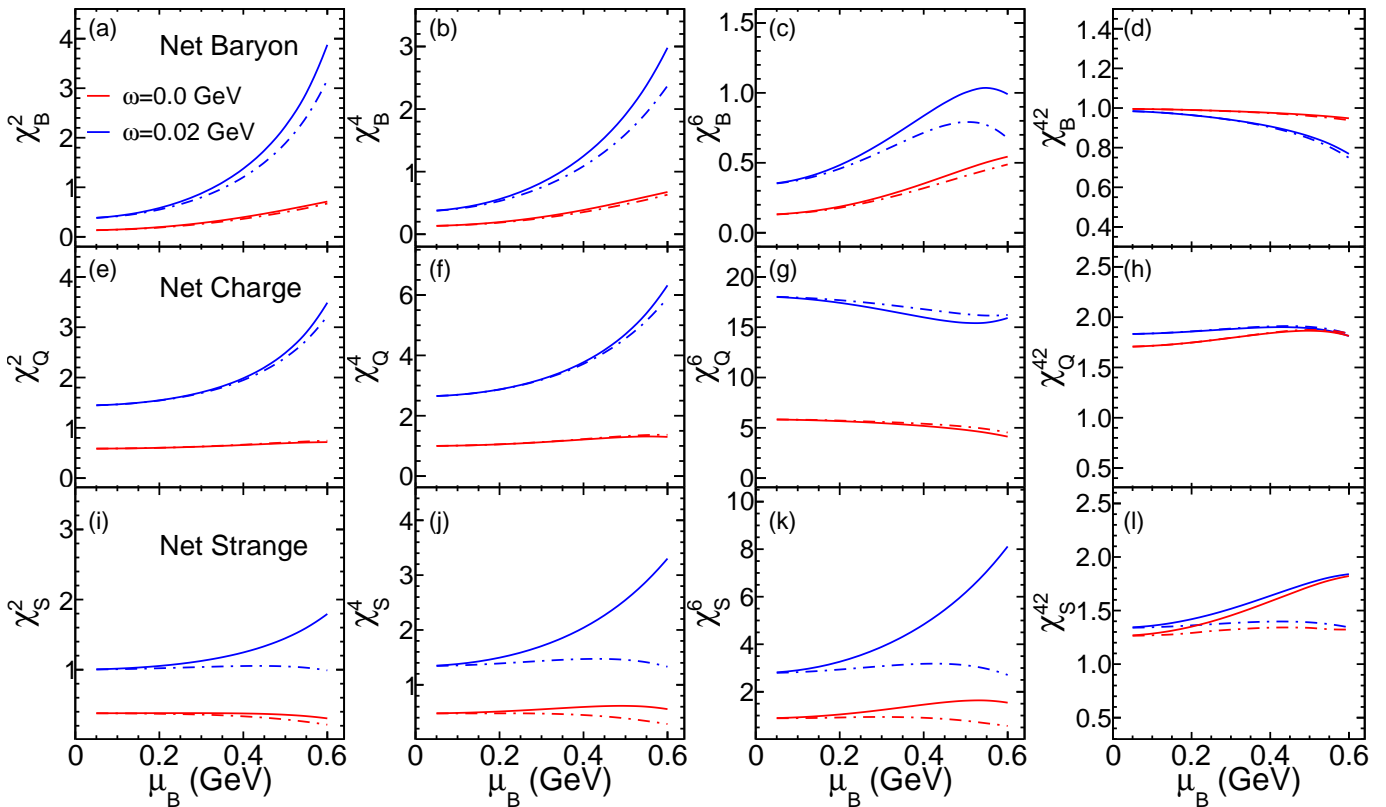


**Fig. 4.** Susceptibilities ( $\chi^2$ ,  $\chi^4$ , and  $\chi^6$ ) and the ratios ( $\chi^{42} = \chi^4/\chi^2$ ) for net-baryon, net-charge and net-strangeness as a function of  $\mu_B$  without (solid line) and with (dashed line) inclusion of rotation.

Products of moments of net-proton, net-charge and net-kaon as functions of the centre-of-mass energy  $\sqrt{s_{NN}}$  for central heavy-ion collisions (0 – 5%) at different angular velocity  $\omega$  are shown in the Fig. 5. In order to make connections with experiments, the beam energy dependence of the temperature  $T$  and the chemical potentials  $\mu$ 's has to be provided. We used the parametrization of temperature  $T$  and chemical potential  $\mu$ 's with centre-of-mass energy  $\sqrt{s_{NN}}$  along the freeze-out curve following Ref. [32,35]. The values of  $\omega$  considered here are 0.01, 0.015 and 0.02 GeV. Here, the net-proton fluctuations acts as proxy for net-baryon fluctuations and net-kaon acts as proxy for net-strangeness fluctuations. The theoretical estimation of ratios of susceptibilities for different conserved charges are compared with the product of moments for net-proton, net-charge and net-kaon as a function of  $\sqrt{s_{NN}}$  from measured data of STAR [48–50] and HADES [51] experiment. We found that  $(\sigma^2/M)_p$  has insignificant dependence on the rotation  $\omega$ . For  $(S\sigma)_p$  and  $(\kappa\sigma^2)_p$ , the effect of rotation is significant at lower  $\sqrt{s}$  and the ratios decreases with increase of  $\omega$  values. At the higher collision energies, the rotation has no effect on the ratios of net-proton susceptibilities. It should be noted that,  $(\kappa\sigma^2)_p$  with finite rotation for  $\omega = 0.02$  GeV, can explain the data of HADES while normal HRG fails to explain. The  $(\sigma^2/M)_Q$  increases with respect to the center of mass energy for with or without inclusion of rotation. The  $(\sigma^2/M)_Q$  and  $(S\sigma)_Q$  are weakly dependent on

$\omega$  whereas  $(\kappa\sigma^2)_Q$  is insignificant to rotation. In case of  $(\sigma^2/M)_k$ , rotation has small effect at higher  $\sqrt{s_{NN}}$ . For  $(S\sigma)_k$  there is significant and non-monotonic effect of rotation observed at lower collision energies.  $(S\sigma)_k$  values decreases with the increase in rotation.  $(\kappa\sigma^2)_k$  increases with the increase in rotation.

We have also estimated the ratio of susceptibilities for peripheral collisions. From the causality condition  $R\omega \leq 1$ , the values of angular velocity  $\omega$  considered are  $\omega = 0.02, 0.03, 0.04$  GeV for  $r < R = 12.5$  GeV $^{-1}$ . Ratio of susceptibilities from theoretical estimation are compared with product of moments from experimental measurements from STAR [52]. As the freeze-out parametrization used above, was suitable for central collisions, we have used the parameterized values of  $T$ ,  $\mu$ 's at different  $\sqrt{s_{NN}}$  for peripheral collisions (70 – 80%) from Ref. [43]. Figure 6 shows the comparison of theoretical estimation with experimental measurements of the product of moments for the peripheral collisions. We don't observe the effect of rotation for ratios of net-proton number fluctuations for peripheral collisions. The behavior of ratios of the fluctuations for net-electric charge and net-strangeness are in peripheral collisions is completely different from what has been observed for central collisions.  $(\sigma^2/M)_Q$  values increase with  $\sqrt{s_{NN}}$ , but decrease with the increase in rotation, particularly at higher collision energies. In case of  $(S\sigma)_Q$ , at lower collision energies the  $S\sigma$  values increase with increase in rotation and at higher  $\sqrt{s_{NN}}$  the effect of

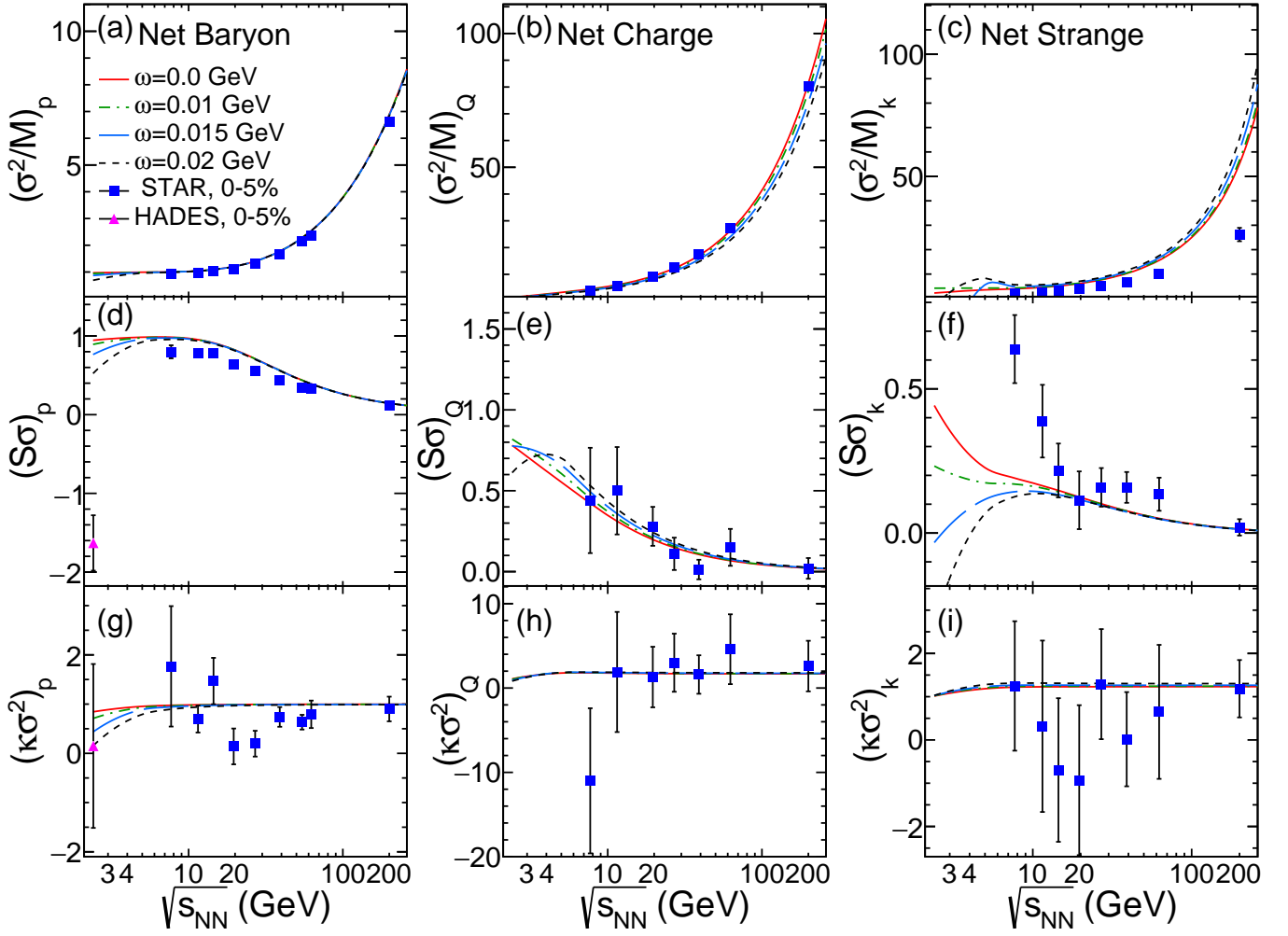


**Fig. 5.** Products of moments of net-proton (left column), net-charge (middle column) and net-kaon (right column) as functions of the centre-of-mass energy for different angular velocity  $\omega$ .

rotation is diminished.  $(\kappa\sigma^2)_Q$  values are independent of rotation. The most pronounced effect is observed in case of net-kaon fluctuations.  $(\sigma^2/M)_k$  values increase with the increase in rotation and the effect is more at higher energies, whereas  $(S\sigma)_k$  values decrease with the increase in rotation values of the system.  $(\kappa\sigma^2)_k$  values increase with the increase in rotation and remain constant for all  $\sqrt{s_{NN}}$ . To summarize the findings in peripheral collisions, it is observed that, the effect of rotation is significant for electric-charge and strangeness but much less so for ratio of susceptibilities for baryon number for the  $\omega$  values considered ( $\omega = 0.02, 0.03, 0.04$  GeV).

We here briefly outline some future directions and potential extension of this work. The ideal HRG model takes into account the attractive interactions between its hadronic constituents via inclusion of resonances and we have analyzed the same idealized system rotating rigidly inside an infinite cylinder. Further refinements to simulate the HIC fireball more realistically, such as including finite size effects in the longitudinal direction, repulsive interactions, inhomogeneity [53], anisotropy, parallel magnetic field [10],

repulsive interactions [54], are possible and can be built upon this work subsequently. In the literature, the possibility of a sequential, flavor-dependent freeze-out has been explored [55]. Considering such a scenario may help in a more refined interpretation of the reported results here leading to a better understanding of the freeze-out process in HICs.

The QCD phase transition in the presence of magnetic field has been studied extensively in the literature. Given the analogous properties of a magnetic field and rotation in the non-relativistic domain and certain similarities in relativistic cases [56] it is interesting, both theoretically and phenomenologically, to consider the possible consequences of having both acting simultaneously as should be the situation in off-central HICs.

## 5 Summary and Conclusion

The fluctuations of conserved numbers, namely net-baryon number, net-strangeness and net-charge were studied using HRG model in the presence of global rotation. We

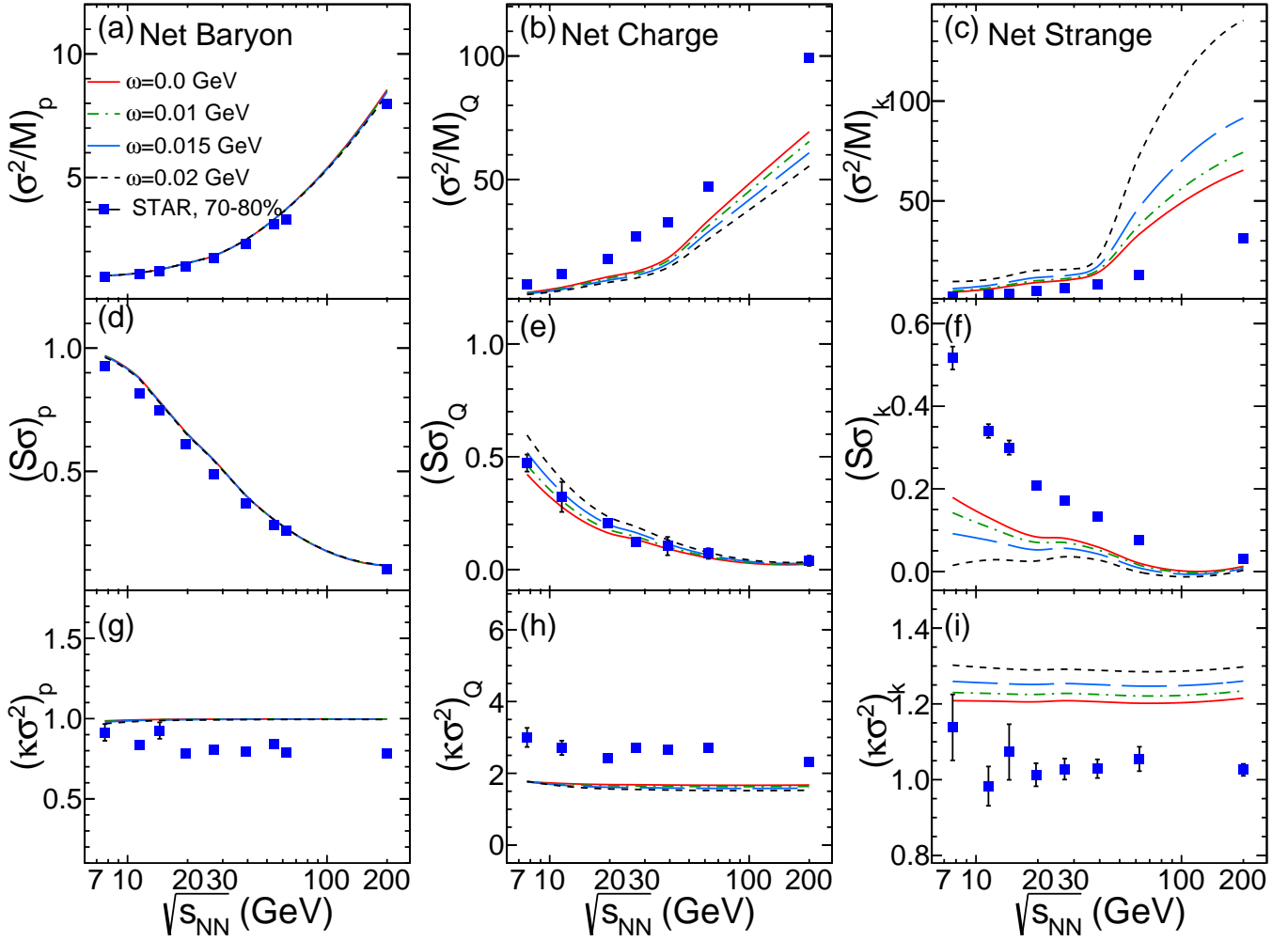


**Fig. 6.** Products of moments of net-proton (left column), net-charge (middle column) and net-kaon (right column) as functions of the centre-of-mass energy for different angular velocity  $\omega$  for peripheral collisions.

have chosen three different values of the angular velocity  $\omega$  for both central and peripheral collisions in the expected range from simulation and measurement at RHIC [2, 6]. This study gives the maximum limit of effect of rotation on the product of moments or fluctuations of conserved charges.

The susceptibilities of baryon number, electric charge and strangeness number are found to be sensitive to rotation. We have studied the behavior of moments as a function of  $\sqrt{s_{NN}}$  using freeze-out parametrization for central collisions for  $\omega = 0$  as well as using parameters estimated for peripheral collisions.  $(S\sigma)_B$  and  $(\kappa\sigma^2)_B$  show a decreasing trend with increasing  $\omega$  at very low centre-of-mass energy which could explain the data of  $(\kappa\sigma^2)_p$  measured with HADES at  $\sqrt{s_{NN}} = 2.4$  GeV. We found that rotation, parameterized by  $\omega$ , has potentially important implications for the interpretation of heavy-ion collision data. In future studies,  $\omega$  may play the role of one of the freeze-out parameters besides  $T$  and  $\mu_B$ .

## References

1. F. Becatini, et al., Euro. Phys. J. C 75 (2015) 406. doi: [10.1140/epjc/s10052-015-3624-1](https://doi.org/10.1140/epjc/s10052-015-3624-1).
2. Y. Jiang, Z.-W. Lin, J. Liao, Phys. Rev. C 94 (2016) 044910. doi: [10.1103/PhysRevC.94.044910](https://doi.org/10.1103/PhysRevC.94.044910).
3. Z. T. Liang, X. N. Wang, Phys. Rev. Lett. 94 (2016) 102301. doi: [10.1103/PhysRevLett.94.102301](https://doi.org/10.1103/PhysRevLett.94.102301).
4. Y. Jiang, J. Liao, Phys. Rev. Lett. 117 (2016) 192302. doi: [10.1103/PhysRevLett.117.192302](https://doi.org/10.1103/PhysRevLett.117.192302).
5. W. T. Deng, X. G. Huang, Phys. Rev. C 93 (2016) 064907. doi: [10.1103/PhysRevC.93.064907](https://doi.org/10.1103/PhysRevC.93.064907).
6. L. Adamczyk, et al., Nature 548 (2017) 62. doi: [10.1038/nature23004](https://doi.org/10.1038/nature23004).
7. Y. Fujimoto, K. Fukushima, Y. Hidaka, Phys. Lett. B 816 (2021) 136184. doi: [10.1016/j.physletb.2021.136184](https://doi.org/10.1016/j.physletb.2021.136184).
8. K. Fukushima, Prog. Part. Nucl. Phys. 107 (2019) 167. doi: [10.1016/j.pnpnp.2019.04.001](https://doi.org/10.1016/j.pnpnp.2019.04.001).
9. F. Becatini, M. A. Lisa, Ann. Rev. Nucl. Part. Sci. 70 (2020) 423. doi: [10.1146/annurev-nucl-021920-095245](https://doi.org/10.1146/annurev-nucl-021920-095245).
10. G. Mukherjee, D. Dutta, D. K. Mishra arXiv: 2304.12643.
11. D. Kharzeev, A. Zhitnitsky, Nucl. Phys. A 797 (2007) 67. doi: [10.1016/j.nuclphysa.2007.10.001](https://doi.org/10.1016/j.nuclphysa.2007.10.001).



12. D. T. Son, P. Surowka, Phys. Rev. Lett. 103 (2009) 191601. doi:10.1103/PhysRevLett.103.191601.
13. D. Kharzeev, D. T. Son, Phys. Rev. Lett. 106 (2011) 062301. doi:10.1103/PhysRevLett.106.062301.
14. Y. Jiang, X. G. Huang, J. Liao, Phys. Rev. D 92 (2015) 071501. doi:10.1103/PhysRevD.92.071501.
15. S. Ebihara, K. Fukushima, K. Mameda, Phys. Lett. B 764 (2017) 94. doi:10.1016/j.physletb.2016.11.010.
16. A. Yamamoto, Y. Hirono, Phys. Rev. Lett. 111 (2013) 081601. doi:10.1103/PhysRevLett.111.081601.
17. V. V. Braguta, A. Y. Kotov, D. D. Kuznedev, A. A. Roenko, JETP Lett. 112 (2020) 6. doi:10.31857/S1234567820130029.
18. Y. Aoki, Z. Fodor, S. D. Katz, K. K. Szabo, Phys. Lett. B 643 (2006) 46. doi:10.1016/j.physletb.2006.10.021.
19. Y. Aoki, G. Endrodi, Z. Fodor, S. D. Katz, K. K. Szabo, Nature 443 (2006) 675. doi:10.1038/nature05120.
20. S. Borsanyi, Others, Phys. Rev. D 92 (2015) 014505. doi:10.1103/PhysRevD.92.014505.
21. P. Peterczky, AIP Conf. Proc. 1520 (2013) 103. doi:10.1063/1.4795947.
22. B. Friman, C. Hohne, J. Knoll, S. Leupold, J. Randrup, R. Rapp, P. Senger, Lect. Notes Phys. 814 (2011) 1. doi:10.1007/978-3-642-13293-3\_2.
23. M. Asakawa, K. Yazaki, Nucl. Phys. A 504 (1989) 668. doi:10.1016/0375-9474(89)90002-X.
24. A. Barducci, R. Casalbouni, S. D. Curtis, R. Gatto, G. Pettini, Phys. Rev. D 41 (1990) 1610. doi:10.1103/PhysRevD.41.1610.
25. J. Berges, K. Rajagopal, Nucl. Phys. B 538 (1999) 215. doi:10.1016/S0550-3213(98)00620-8.
26. S. Ejiri, F. Karsch, K. Redlich, Phys. Lett. B 633 (2006) 275. doi:10.1016/j.physletb.2005.11.083.
27. M. A. Stephanov, K. Rajagopal, E. V. Shuryak, Phys. Rev. D 60 (1999) 114028. doi:10.1103/PhysRevD.60.114028.
28. A. Bzdak, S. Esumi, V. Koch, J. Liao, M. Stephanov, N. Xu, Phys. Rep. 853 (2020) 1. doi:10.1016/j.physrep.2020.01.005.
29. F. Karsch, Moments of charge fluctuations, pseudo-critical temperatures and freeze-out in heavy-ion collisions, Journal of Physics G: Nuclear and Particle Physics 38 (12) (2011) 124098. doi:10.1088/0954-3899/38/12/124098. URL <https://dx.doi.org/10.1088/0954-3899/38/12/124098>
30. S. Gupta, X. Luo, B. Mohanty, H. G. Ritter, N. Xu, Science 332 (2011) 1525. doi:10.1126/science.1204621.
31. R. V. Gavai, S. Gupta, Phys. Lett. B 696 (2011) 459. doi:10.1016/j.physletb.2011.01.006.
32. F. Karsch, K. Redlich, Phys. Lett. B 695 (2011) 136. doi:10.1016/j.physletb.2010.10.046.
33. P. Garg, D. K. Mishra, Phys. Rev. C 96 (2017) 044908. doi:10.1103/PhysRevC.96.044908.
34. P. Garg, D. K. Mishra, P. K. Netrakanti, B. Mohanty, A. K. Mohanty, B. K. Singh, Phys. Lett. B 726 (2013) 691. doi:10.1016/j.physletb.2013.09.019.
35. J. Cleymans, H. Oeschler, K. Redlich, S. Wheaton, Phys. Rev. C 73 (2006) 034905. doi:10.1103/PhysRevC.73.034905.
36. P. Barun-Mumzinger, J. Stachel, J. P. Wessels, N. Xu, Phys. Lett. B 344 (1995) 43. doi:10.1016/0370-2693(94)01534-J.
37. J. Cleymans, D. Elliott, H. Satz, R. L. Thews, Z. Phys. C 74 (1997) 319. doi:10.1007/s002880050393.
38. G. Kadam, S. Pal, A. Bhattacharyya, J. Phys. G Nucl. Part. Phys. 47 (2020) 125106. doi:10.1088/1361-6471/abba70.
39. S. Gupta, D. Mallick, D. K. Mishra, B. Mohanty, N. Xu, Phys. Lett. B 829 (2022) 137021. doi:10.1016/j.physletb.2022.137021.
40. K. A. Olive, et al., Rev. Part. Phys. C 38 (2014) 090001. doi:10.1088/1674-1137/38/9/090001.
41. A. Bazavov, et al., Equation of state in (2+1)-flavor QCD, Phys. Rev. D 90 (2014) 094503. arXiv:1407.6387, doi:10.1103/PhysRevD.90.094503.
42. S. Borsanyi, Z. Fodor, C. Hoelbling, S. D. Katz, S. Krieg, K. K. Szabo, Full result for the QCD equation of state with 2+1 flavors, Phys. Lett. B 730 (2014) 99–104. arXiv:1309.5258, doi:10.1016/j.physletb.2014.01.007.
43. L. Adamczyk, et al., Phys. Rev. C 96 (2017) 044904. doi:10.1103/PhysRevC.96.044904.
44. A. Bhattacharyya, S. K. Ghosh, R. Ray, S. Samanta, EPL 115 (2016) 62003. doi:10.1209/0295-5075/115/62003.
45. B. Aboona, et al., Phys. Rev. Lett. 130 (8) (2023) 082301. doi:10.1103/PhysRevLett.130.082301.
46. A. Bazavov, et al., Phys. Rev. D 101 (7) (2020) 074502. doi:10.1103/PhysRevD.101.074502.
47. B. Friman, F. Karsch, K. Redlich, V. Skokov, Fluctuations as probe of the QCD phase transition and freeze-out in heavy ion collisions at LHC and RHIC, Eur. Phys. J. C 71 (2011) 1694. arXiv:1103.3511, doi:10.1140/epjc/s10052-011-1694-2.
48. L. Adamczyk, et al., Phys. Rev. Lett. 113 (2014) 092301. doi:10.1103/PhysRevLett.113.092301.
49. M. S. Abdallah, et al., Phys. Rev. Lett. 127 (2021) 262301. doi:10.1103/PhysRevLett.127.262301.
50. L. Adamczyk, et al., Phys. Lett. B 785 (2018) 551–560. arXiv:1709.00773, doi:10.1016/j.physletb.2018.07.066.
51. J. Adamczewski-Musch, et al., Phys. Rev. C 102 (2020) 024914. doi:10.1103/PhysRevC.102.024914.
52. J. Adam, et al., Phys. Rev. Lett. 126 (2021) 092301. doi:10.1103/PhysRevLett.126.092301.
53. M. N. Chernodub, Phys. Rev. D 103 (5) (2021) 054027. doi:10.1103/PhysRevD.103.054027.
54. K. K. Pradhan, B. Sahoo, D. Sahu, R. Sahoo, Thermodynamics of a rotating hadron resonance gas with van der Waals interaction arXiv:2304.05190.
55. C. Ratti, Lattice QCD and heavy ion collisions: a review of recent progress, Rept. Prog. Phys. 81 (8) (2018) 084301. arXiv:1804.07810, doi:10.1088/1361-6633/aabb97.
56. K. Mameda, A. Yamamoto, Magnetism and rotation in relativistic field theory, PTEP 2016 (9) (2016) 093B05. arXiv:1504.05826, doi:10.1093/ptep/ptw128.